Biomarkers, 2009; 14(8): 572–586

informa
healthcare

ORIGINAL ARTICLE

A systems biology approach to understanding elevated serum alanine transaminase levels in a clinical trial with ximelagatran

Ulf Andersson[1], Johan Lindberg[1], Shunghuang Wang[2], Raji Balasubramanian[3], Maritha Marcusson-Ståhl[1], Mira Hannula[1], Chenhui Zeng[2], Peter J. Juhasz[2], Johan Kolmert[1], Jonas Bäckström[1], Lars Nord[1], Kerstin Nilsson[4], Steve Martin[2], Björn Glinghammar[1], Karin Cederbrant[1], and Ina Schuppe-Koistinen[1]

[1]Safety Assessment, Molecular Toxicology, AstraZeneca R&D, S-151 85 Södertälje, Sweden, [2]BG Medicine, Waltham, MA 02451, USA, [3]University of Massachusetts, Shrewsbury, MA, USA, and [4]Disease Biology, AstraZeneca R&D, 151 85 Södetälje, Sweden

Abstract

Ximelagatran was developed for the prevention and treatment of thromboembolic conditions. However, in long-term clinical trials with ximelagatran, the liver injury marker, alanine aminotransferase (ALT) increased in some patients. Analysis of plasma samples from 134 patients was carried out using proteomic and metabolomic platforms, with the aim of finding predictive biomarkers to explain the ALT elevation. Analytes that were changed after ximelagatran treatment included 3-hydroxybutyrate, pyruvic acid, CSF1R, Gc-globulin, L-glutamine, protein S and alanine, etc. Two of these analytes (pyruvic acid and CSF1R) were studied further in human cell cultures *in vitro* with ximelagatran. A systems biology approach applied in this study proved to be successful in generating new hypotheses for an unknown mechanism of toxicity.

Keywords: *Liver injury; systems biology; alanine aminotransferase; pyruvate; ximelagatran*

Introduction

Despite rigorous preclinical studies, hepatotoxicity is one of the most important adverse drug reactions in humans leading to non-approval, limitations in use or withdrawal of drugs from the market (Lee 2003). Ximelagatran, an oral direct thrombin inhibitor marketed as Exanta®, was developed for the prevention and treatment of thromboembolic conditions. However, elevated alanine aminotransferase (ALT) levels were observed in patients treated for more than 35 days with ximelagatran (Lee et al. 2005). The ALT elevation (ALT >3 x upper limit of normal (ULN)) typically occurred between 1 and 6 months after initiation of treatment in 6–13% (mean 7.9%) of patients and returned to normal in most patients within 6 months, whether or not treatment was continued. Ximelagatran was withdrawn from the market and its development terminated in 2006 (McCaffrey & Brown 2006).

The underlying mechanisms of these ALT elevations in some of the patients are not known. The preclinical toxicology programme, performed on a variety of species including the cynomolgus monkey with repeated administration of ximelagatran (or the active form: melagatran), did not reveal adverse histopathology or increased serum ALT indicating hepatotoxic effects. An extensive programme was performed to investigate the mechanism of ALT elevation using both clinical and preclinical studies including a retrospective case–control pharmacogenetics study (Kindmark et al. 2008) and a panel of *in vitro* studies (Kenne et al. 2008).

Systems biology has developed in recent years into a promising tool in drug research and development

Address for Correspondence: Ulf Andersson, Safety Assessment Södertälje, B691, AstraZeneca R&D, SE-151 85 Södertälje, Sweden. E-mail: ulf.s.andersson@astrazeneca.com

(Received 27 May 2009; revised 13 August 2009; accepted 14 August 2009)

ISSN 1354-750X print/ISSN 1366-5804 online © 2009 Informa UK Ltd
DOI: 10.3109/13547500903261354

for understanding disease biology and effects of drug treatment (van der Greef et al. 2007). A suitable application for this approach is in the area of problem solving in safety assessment to provide molecular entry points into an observation of unknown mechanism. To gain insights into the biological processes that contribute to a patient's predisposition to developing ALT elevation, an integrated systems toxicology approach was taken to study plasma samples from a subset of patients treated with ximelagatran in the clinical trial SPORTIF (Stroke Prevention using an oral thrombin inhibitor in atrial fibrillation) III (Olsson 2003). These samples included both pre-dose and treatment time points for patients who did not develop ALT elevation upon treatment (controls) as well as those who developed ALT elevation upon treatment (cases). Plasma protein levels were measured using iTRAQ liquid chromatography/mass spectrometry/mass spectrometry (LC/MS/MS) proteomics. Plasma metabolites including lipids and polar analytes were measured using LC/MS/MS, gas chromatography (GC)/MS, and nuclear magnetic resonance spectroscopy (NMR).

The subsequent integrated statistical analysis resulted in a set of putative predisposition biomarkers for ALT elevation after ximelagatran treatment and a set of putative treatment-effect biomarkers. This article describes the results from the systems toxicology study performed on human plasma samples from a phase III clinical trial and presents two hypotheses for predisposition and mechanisms involved in transient elevations of serum ALT elevations in ximelagatran-treated patients. Results are also presented from *in vitro* and *ex vivo* experiments performed to investigate the hypotheses generated from the systems biology data.

Materials and methods

Study population

A total of 140 selected patients diagnosed with atrial fibrillation in the SPORTIF III clinical trial were available for analysis (Olsson 2003). Forty-six of these subjects developed ALT elevation >3 x ULN, during treatment (these were designated cases), while 94 did not and these were designated controls. Samples were taken at one of the following four occasions: (1) pre-dose (sample taken at study entry); (2) pre-ALT-peak; (3) at-ALT-peak; or (4) post-ALT-peak. Of the 46 subjects with significant ALT elevations (cases), 34 had maximum ALT levels in the range 3–9 x ULN and 12 subjects had maximum ALT levels ≥9 x ULN. Eight subjects with equivocal ALT elevations were subsequently excluded from analysis giving a total of 134 analysed patients. For discovery of putative treatment-effect biomarkers, selection of subjects for data analysis and interpretation was restricted to those subjects who had a pre-dose measurement, body mass index (BMI) <30 and ALT levels >3 x ULN either a pre-peak ALT or at-peak ALT measurement. Post-peak ALT measurements were not included in the data analysis due to the uncertainty as to whether these subjects were still on ximelagatran treatment when these samples were drawn. The above selection criteria resulted in 13 subjects being included in the analysis. An independent Research Ethics Committee, the Regional Ethical Review Board, Department of Medicine in Gothenburg, Sweden, approved the study. All plasma samples were anonymised prior to analysis to preserve patient confidentiality.

Plasma samples

Venous blood samples from the SPORTIF III clinical trial (Olsson 2003) were collected in citrate sampling tubes. If a catheter was used, the first 1 ml of blood was discarded. Plasma was prepared within 1 h of blood sampling by centrifugation at 2000*g* for 20 min and immediately frozen and stored below –20°C.

Analytical workflow

The general work flow for all analytical platforms was: (1) Sample preparation and extraction, (2) data acquisition, (3) quality control (QC) of individual samples and batch data, (4) peak detection and integration, (5) scaling and normalization, (6) univariate and multivariate data analysis.

Analytical platforms

^{1}H NMR platform

Two hundred and fifty microlitres of plasma was diluted with 330 µl D_2O. Low-molecular weight metabolites were detected with a Bruker 600 MHz Avance NMR (Bruker, Billerica, MA, USA) spectroscopy instrument using a standard ^{1}H 1D NOESY-presat pulse sequence.

Lipid platform

Two hundred microlitres of extraction solution (1:9 ratio of dichloromethane/isopropyl alcohol) was added to 10 µl of plasma. A Waters 2795 Alliance high-performance LC (HPLC) system (Waters, Milford, MA, USA) coupled with a Symmetry C4 column (300 Å, 3.5 µm, 2.1 x 150 mm) was used at a flow rate of 350 µl min^{-1} with the following gradient: 0–2 min 20% B, 2–4 min 20–80% B, 4–20 min 80–100% B, 20–25 min isocratic at 100% B and then returning to 20% B for 10 min equilibration. Solvent A comprised 95% H_2O and 5% MeOH and solvent B comprised 99% MeOH and 1% H_2O. Both solvent streams contained 10 mM ammonium acetate and 0.1% formic acid. Data were acquired, *m/z* 300–1000, using

a Waters/Micromass quadrupole time-of-flight instrument (Q-ToF) equipped with a LockSpray electrospray ionization (ESI) source.

HPLC polar

Ten microlitres of internal standard mix solution was added to 10 µl plasma and deproteinized with methanol. The samples were then derivatized with HCl–butanol at 65°C and reverse phase separated using a Surveyor Plus HPLC (Thermo Fischer Scientific, Waltham, MA, USA). Data were acquired, *m/z* 125–1250, using a LTQ ion trap mass spectrometer (Thermo Fischer Scientific) coupled with an ESI source operated in positive ion mode (Davidov et al. 2004).

UPLC polar

Sixty microlitres of plasma was precipitated with 350 µl methanol. Analytes were separated using an ultraperformance LC (UPLC) system equipped with a reversed-phase BEH C18 (2.1 x 100 mm, 1.7 µm) column (Waters). Mobile phases A1 (0.1% aqueous formic acid) and B1 (0.1% formic acid in acetonitrile) were used for sample elution at 600 µl min^{-1}, gradient started with 0–5.5 min 1–20% B followed by 5.5–9 min 20–100% B; B2 (0.1% formic acid in methanol) for 2.5 min was used for washing the column between injections. Total run time was 17.5 min including column equilibration. Data were acquired, *m/z* 80–1000, using a Waters LCT Premier mass spectrometer equipped with a LockSpray ESI source operated in both positive and negative ion mode.

GC/MS polar

An Agilent 6890 N gas chromatograph (Agilent, Palto Alto, CA, USA) was coupled to an Agilent 5973 Mass Selective Detector and 400 µl methanol with internal standards was added to 10 µl of plasma. The samples were subjected to oximation with 30 µl ethoxyamine hydrochloride followed by silylation with *N*-methyl-*N*-trimethylsilyl trifluoroacetamide (Koek et al. 2006). Data were acquired using electron impact (EI) in the mass range *m/z* 300–1000.

Proteomics

The proteomics workflow consisted of abundant protein depletion using a IgY 12-LC10 Column (Beckman Coulter, Fullerton, CA, USA) followed by tryptic digestion and iTRAQ-labelling and 4-plex iTRAQ-labelling (Applied Biosystems, Foster City, CA, USA). (Ross et al. 2004). Once the samples were labelled, three study samples and one QC sample were pooled into a single tube. Each iTRAQ mixture was then fractionated by SCX-chromatography (4.6 x 50 mm Poly-Sulfoethyl Strong Cation Exchange Column) to yield six fractions. Each fraction was analysed (HPLC MALDI MS and MS/MS) using an UltiMate chromatography system equipped with Probot MALDI spotter (Dionex-LC Packings, Hercules, CA, USA). An internal standard peptide (ACTH 18-39; MH^+=2465.199) was added to the matrix solution (10 mg ml^{-1} α-cyano-4-hydroxycinnamic acid/0.1 g l^{-1} dibasic ammonium citrate in 15% water, 85% acetonitrile, 1:1 ratio to sample flow). Loading buffer was 95% water, 5% acetonitrile, 0.1% TFA, 2 mM ammonium acetate for the C18 trap column, 0.3 x 5 mm (Dionex-LC Packings). Mobile phase A consisted of 95% water, 5% acetonitrile, 0.1% TFA and mobile phase B 10% water, 90% acetonitrile, 0.1% TFA. For the analytical C18 column, 0.180 x 150 mm (Dionex-LC Packings) a gradient with flow rate of 2 µl min^{-1} was used as follows: 5% B for 8 min, 5–11% B in 35 min, 38–100% in 2 min and then held isocratic for 1 min. MALDI mass spectrometry data was recorded using the MDS Sciex/Appplied Biosystems 4800 Mass Analyzer over the *m/z* range 500–4500. Two internal standards were used for mass calibration: *m/z* 2465.199 (peptide standard co-infused with the matrix) and *m/z* 568.136 (matrix trimer). After MS acquisition for each sample (two plates) an inhouse-developed procedure was used to select precursors for MS/MS acquisition. Peptide identification was done by Mascot (MatrixScience Ltd., London, UK), searched according to the following: precursor mass tolerance 200 ppm, fragment mass tolerance 0.4 Da, enzyme specificity fully tryptic, variable modifications; N-term iTRAQ, lysine iTRAQ, Cys carbamidomethyl, pyro-Glu (N-term), pyro-carbamidomethyl Cys (N-term), de-amidation (N only) and oxidation (M), two missed tryptic sites and considering only peptide rank 1. Further, an autovalidation step as well as manual was then used for assigning protein and peptide identities. An inhouse database allowed the curation of the Mascot results.

For quantification, sample-specific normalization factors were estimated from a subset of 'stable' peptides that were chosen based on methods previously described (Vandesompele et al. 2002). All pairs of peptides were evaluated for stability of peptide ratios across samples – those peptides with high levels of stability (or low variability) were chosen as 'stable peptides'. Moreover, all 'stable peptides' had low levels of missing values across all samples (less than 10%). Data from 133 'stable peptides' were treated as internal standards and used to estimate sample-specific normalization factors. All peptide ratios measured from the same sample were scaled to the same normalization factor.

Scaling and normalisation

For the lipid, polar and GC/MS platforms the samples were normalized and batch corrected using a series of internal standards and external quality control

samples. Taking an aliquot of each study sample and combining those materials in a pool created the external QC sample. This QC sample was used multiple times per batch for all platforms described above. In the metabolomic platforms the QC pool samples were analysed as external standards while in the proteomics analysis they were run as internal control samples. In the metabolomic platforms each analyte was normalized against the internal standard providing the lowest CV in the QC sample data across all batches, i.e each analyte was quoted against the internal standard best mapping the analyte variance pattern in the QC data. Following quoting, a batch-wise linear trend correction were used in conjunction with an off-set multiplication. Three to nine deuterized endogenous analytes and/or exogenous analytes were used as internal standards for the polar platforms. For the NMR platform no normalization was needed due to low analyte variance in the QC samples. The normalization steps and other statistical operations were performed using Matlab® software (Mathworks, Natick, MA, USA).

Multivariate analysis

The multivariate classification procedure, Random Forest (Breiman 2001) was used to seek an optimal minimum set of analytes measured at the pre-dose time point that can predict development of ALT elevation during the course of treatment with ximelagatran. The optimal minimum classifier was based on the number of analytes (i.e. K_{opt}) that minimized the overall error rate, estimated via external cross-validation (Ambroise & McLachlan 2002). The final classifier was derived by recursive feature elimination until the desired number of analytes remained in the classifier. As shown in Table 1, the samples were distributed unevenly across different states and categories. The imbalance in the sample distribution across groups resulted in poorer precision in classifying subjects in the smaller groups at the expense of better precision in classifying subjects in the larger group. To strike a balance in the trade-off between sensitivity and specificity, the Random Forest classifier was run by specifying that equal numbers of cases and controls to be randomly sampled for each tree, thus adjusting for the imbalance in the sample distribution across groups (via the 'sample size' option in the algorithm implemented in R). In each analysis, the number of cases (and controls) was chosen to equal 0.75 x Nc, where Nc is the number of cases.

The variable importance measures, defined as the decrease in prediction accuracy upon random permutations of each analyte, were obtained from the final classifier built from Kopt analytes. Finally, a *p*-value denoting the statistical significance of each multivariate classifier was calculated based on 25 random permutations of the case–control labels associated with each subject.

Univariate analysis

Logistic regression models were used to discover putative biomarkers of predisposition to developing ALT elevation. Two models were developed for each analyte individually. Model 1 included as covariates the main effects of gender, BMI (< 30 vs > 30) and the analyte intensity (transformed to the natural logarithm scale). Model 2 included all main effects terms in model 1 as well as two two-way interaction terms – namely, the interaction between analyte intensity and gender and the interaction between analyte intensity and BMI. A *p*-value was calculated for each analyte and model based on likelihood ratio tests of the comparison of each model to a nested null model constructed without the terms involving the analyte. *p*-Values were reported based on model 1 for the proteomics, NMR and lipid LC/MS platforms – this was based on the observation that the *p*-values from both models were very similar for these platforms. For all other platforms, *p*-values were reported based on model 2 – this was driven by evidence of a larger number of statistically significant findings from model 2 when compared with model 1.

In order to control the false discovery rate (FDR) among all significant findings, the method of Benjamini and Hochberg (1995) was applied. FDR-adjusted *p*-values were calculated based on the raw *p*-values for 1184 analytes measured across all platforms. The integrated putative predisposition biomarkers were chosen using an FDR-adjusted *p*-value threshold of 0.3 and a corresponding raw *p*-value threshold of 0.02.

The set of analytes chosen as putative biomarkers may be significant predictors of predisposition to ALT elevation in one gender BMI category, but not in the other. In order to determine the categories in which each biomarker acts as a significant predictor, category-specific Wald test *p*-values were calculated for every putative biomarker (Wald 1949). Because the univariate model used in the proteomics, NMR and lipid LC/MS platforms assumed constant odds ratios (OR) across categories (i.e. model 1), category-specific *p*-values were rendered irrelevant for these platforms.

For a given category, the OR *R* for a given predisposition biomarker implied that the odds of developing ALT elevation for a subject with x +1 units (natural log scale) of the analyte is *R* times the odds for a similar individual with x units (natural log scale) of the same analyte. Hence an OR >1 means that a higher level of the biomarker predisposed a patient to the development of ALT elevation, while an OR <1 indicates a protective effect against ALT elevation of higher concentration of the biomarker.

To discover putative treatment-effect biomarkers, paired *t* and one-sample Wilcoxon tests were used to calculate the raw *p*-values to test the mean differences in the levels of analytes between the treated and the pre-dose time points in 13 subjects who developed ALT elevation upon ximelagatran treatment. Analytes that satisfied an FDR-adjusted *p*-value ≤0.2 for both the paired *t*-test and the Wilcoxon test were included in the list of putative treatment-effect biomarkers.

Cell culture and cytotoxicity measurements

Cultures of primary human hepatocytes and hepatoma cells were used to test the hypothesis that cell culture medium deficient in pyruvate could sensitize cells for ximelagatran-induced cytotoxicity. For adenosine triphosphate (ATP) measurements, cryopreserved primary human hepatocytes from two different donors (IZG and GIU) were obtained from In Vitro Technologies (Baltimore, MD, USA). The cells were plated in 200 µl medium (MEM supplemented with, in final concentration: 20% FBS, 500 µM glutamine, 1% non-essential amino acids, 100 U ml^{-1} penicillin, 100 µg ml^{-1} streptomycin and either 0, 50 or 500 µM pyruvate) in white collagen-coated 96-well plates at a density of 20 000 cells per well and kept at 37°C under normal atmospheric oxygen conditions (21%) and 5% CO_2 for 24 h before addition of test compound. Total ATP was assayed using CellTiter-Glo® Luminescent Cell Viability Assay (Promega Biotech AB, Stockholm, Sweden). The assay was performed according to the manufacturer's instructions after 24 or 48 h of incubation with test compounds. HepG2, (ATCC) were cultured in MEM (supplemented with and either 0 or 500 µM pyruvate) in collagen-coated bottles. At confluence, cells were detached by trypsin/EDTA (0.05% trypsin with EDTA) and replated with a subcultivation ratio of 1:3–1:5. Cells were kept at 37°C under normal oxygen conditions and 5% CO_2. For experiments using lactate dehydrogenase (LDH) activity in the medium as the cytotoxicity marker, cells were plated in 200 µl medium containing either 0 or 500 µM pyruvate in white collagen-coated 96-well plates at a density of 10 000 or 15 000 cells per well, and ximelagatran was added 6 h following plating. Tests were performed after 48 and 96 h with test compounds. For the 96-h time point, the medium and test compound were replaced at 48 h. LDH release into the extracellular fluid was colometrically determined using the commercially available Cytotoxicity Detection Kit (LDH) (Roche Diagnostics, Scandinavia, Bromma, Sweden). According to the manufacturer's protocol, 100 µl of the supernatant of each well was analysed after 48 and 96 h. Total protein was quantified with BCA™ Protein Assay Kit (Nordic Biolabs AB, Täby, Sweden). Total amount of protein was used for normalization of data from LDH measurements.

For cytotoxicity experiments using propidium iodide (PI), 150 000 HepG2 cells were plated in 24-well plates and cultured in MEM with either 0 or 500 µM pyruvate. After 24 h of plating, cells were treated with ximelagatran (30 and 300 µM) and a positive control for cell death, tributyltin (TBT, 50 nM) for 48 h. All cells in the medium and cells attached into the wells were then removed by a short trypsin/EDTA treatment. The number of viable cells ml^{-1} (total number of cells – PI stained cells) in all wells were counted in a NucleoCounter® (ChemoMetec A/S, Allerod, Denmark). The number of observations per treatment was four.

CSF1R and HLA-DR expression on in vitro*-activated monocytes isolated from human peripheral blood*

Peripheral blood was collected from ten different donors, five males and five females. Monocytes were isolated with RosetteSep® human monocyte enrichment cocktail (StemCell Technologies, Sheffield, UK) according to the description of the manufacturer.

The cells were cultured in RPMI 1640 supplemented with 10 mM Hepes, 4 mM L-glutamine, gentamycin (8 mg ml^{-1}) and 10% AB^+ at a density of 5×10^5 cells per well in 24-well plates and kept at 37°C, 5% CO_2 and 90% humidity. Analysis occurred after 20 and 44 h of incubation with ximelagatran or lipopolysaccharide (LPS) 50 ng ml^{-1}.

After each incubation time, cells were transferred to tubes and stained with fluorochrome-conjugated α-human antibodies: colony-stimulating factor 1 receptor (CSF1R), HLA-DR and CD14 (LPS-receptor). The cells were analysed in a flow cytometer with respect to the mean fluorescence intensity (MFI), this value correlates with the amount expressed CSF1R, HLA-DR or CD14 on the cell surface. The test results are expressed as a percentage of the control (MFI in ximelagatran-treated cultures/MFI in vehicle-treated cultures).

Results

A multivariate model was used in order to find a separation of analytes with regard to ALT elevations in the patients. For this purpose, the Random Forest classifier was used to find an optimal minimum multivariate fingerprint that separates pre-dose controls from pre-dose cases across all gender/BMI categories. This analysis included 93 controls and 41 cases and used 1223 analytes measured in all metabolomics and proteomics platforms. The resulting classifier had 33% classification error with $p = 0.12$, hence no statistically significant multivariate fingerprint across all gender/BMI categories was obtained after adjusting the imbalance in class sizes. A statistically significant multivariate fingerprint was only obtained for

the male/low-BMI category, which was the largest category with 49 controls and 22 cases. The resulting classifier had 29% classification error with $p < 0.001$. The specificity of the classifier was 85% and sensitivity 41%. Because it was not possible to generate a significant classifier in both genders this analytical approach was not further used.

Univariate analysis was used with the aim of searching for predisposition biomarkers for the ALT elevation in patients treated with ximelagatran. Samples from 134 patients for whom pre-dose samples were available were analysed for metabolites and proteins (Table 1). A logistic regression model was used to discover predisposition biomarkers and the raw p-value for the probability of developing an ALT elevation was calculated for each analyte based on a likelihood ratio test. For metabolites measured in the metabolomics platforms (with the exception of the NMR and lipid LC/MS platforms), statistically significant predisposition biomarkers were discovered after taking both gender and BMI into consideration. Examples of analytes that fulfilled the statistical criteria of predisposition biomarkers were kininogen 1 (KNG1), formate, L-cystine, creatinine, lecithin-cholesterol acyltransferase (LCAT), glutamic acid, pyruvic acid, alanine, 2-ketoglutaric acid, apolipoprotein (APO) A2, APOA4, APOE (Table 2).

Next, to discover putative treatment-effect biomarkers, the selection of patients for data analysis and interpretation was restricted to only those subjects who had a BMI <30 and a maximum ALT level >3 x ULN ($n = 13$). Raw p-values were calculated for each analyte based on paired t-tests. p-Values based on the differences in analyte abundance levels between the treated and pre-dose time points were calculated to accommodate the longitudinal nature of the data. Examples of analytes that fulfilled the statistical criteria of treatment biomarkers were 3-hydroxybutyrate, pyruvic acid, L-glutamine, vitamin E, protein S (PROS) 1, CSF1R, C4BPA, Gc-globulin, L-phenylalanine, tyrosine, and a number of mono- and triglycerides (TG) (Table 3).

Hypothesis testing

The metabolite and protein profiling data presented above have been used for the generation of several hypotheses for both predisposition and treatment effects of the compound that could aid in understanding the mechanism behind the observed plasma ALT elevations.

Table 1. Distribution of the 134 pre-dose samples across categories and states.

		Male	Female
BMI <30 (low)	Control	49	27
	Case	22	13
BMI >30 (high)	Control	9	8
	Case	5	1

BMI, body mass index.

The immunological hypothesis

The first hypothesis is based on the finding that in the treatment subgroup (Table 3) the concentration in plasma of CSF1R and Gc-globulin was significantly changed. In addition, the plasma level of C4BPA increased 19% and PROS1 increased about 26% upon ximelagatran treatment. C4BPA and PROS1 positively correlated with each other in the states of pre-dose control ($r = 0.682$, $p < 0.0001$), pre-dose case ($r = 0.776$, $p < 0.0001$) and treated case ($r = 0.591$, $p < 0.0001$). Based on the above findings, possible effects of ximelagatran on monocyte/macrophage activation were analysed *in vitro*. Down-modulation of CSF1R after treatment with monocyte/macrophage activators occurs as a consequence of shedding of CSF1R from the monocyte/macrophage surface. When primary human monocytes/macrophages were stained with the fluorochrome-conjugated α-human CSFR1 antibody a decrease of the fluorescence intensity could be

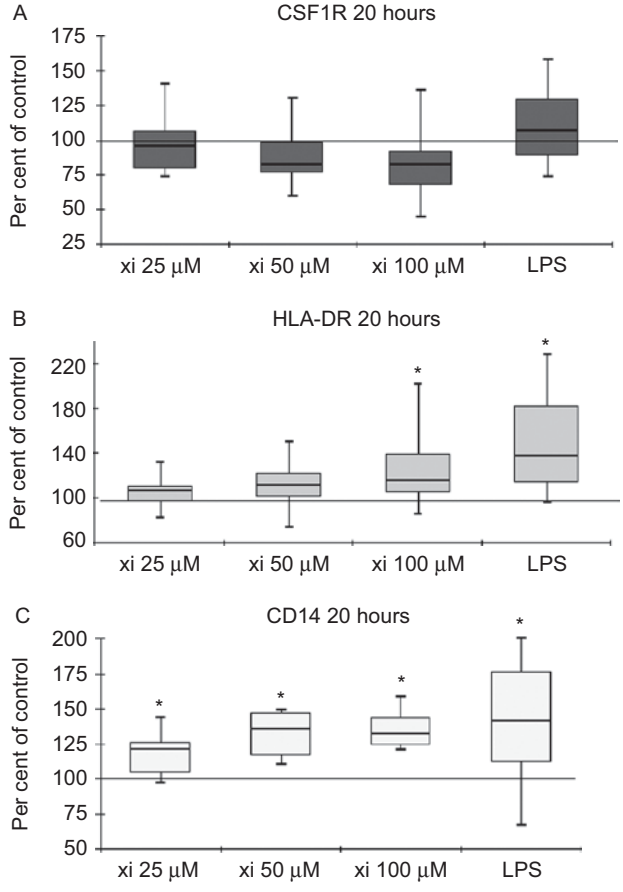

Figure 1. Colony-stimulating factor 1 receptor (CSF1R) (A), HLA-DR (B) and CD14 (C) expression on ximelagatran (Xi)-treated monocytes isolated from human peripheral blood. Data are presented as box-whisker plots where the lower and higher limits of the box are 25% confidence intervals, the whiskers represents the min. and max. value and the line represents the median of the mean fluorescence intensity. *Statistically different from the control, $p < 0.05$. LPS, lipopolysaccharide.

Table 2. Putative predisposition biomarkers from univariate analysis of data from all analytical platforms.

				Male/low BMI			Female/low BMI			
Identification	Platform	Raw *p*	FDR *p*	OR[a]	*p*	MFC[b]	OR	*p*	MFC	CV[c]
KNG1	Prot	0.00	0.03	0.16	NA	0.74	0.16	NA	0.77	NA
Unidentified	P-LC/MS	0.00	0.04	1.10	0.93	0.98	0.00	0.01	0.83	18.28
Formate	NMR	0.00	0.07	13.62	NA	1.10	13.62	NA	1.12	4.08
SERPINF2	Prot	0.00	0.08	0.00	NA	0.89	0.00	NA	0.98	NA
L-Cystine	GC/MS	0.00	0.11	0.18	0.00	0.73	1.01	0.98	0.85	41.11
VTN	Prot	0.00	0.14	0.01	NA	0.86	0.01	NA	0.95	NA
36:4 PE	Lipid LC/MS	0.00	0.14	10.96	NA	1.12	10.96	NA	1.37	12.21
Creatinine	GC/MS	0.00	0.14	0.25	0.15	0.92	4.27	0.23	1.03	8.75
Creatinine	GC/MS	0.00	0.14	0.18	0.09	0.89	4.59	0.19	1.04	7.97
LCAT	Prot	0.00	0.15	257.21	NA	1.08	257.21	NA	1.04	NA
Neuraminic acid	P-LC/MS	0.00	0.18	0.70	0.60	0.91	0.00	0.01	0.76	28.18
Lipid related	NMR	0.00	0.18	0.07	NA	0.97	0.07	NA	0.93	2.54
Unidentified	GC/MS	0.00	0.18	4.18	0.15	1.14	0.00	0.01	0.76	4.08
DL-α-Aminoadipic acid	GC/MS	0.00	0.18	0.33	0.09	0.81	1.10	0.91	0.99	7.35
Fibronectin 1 variant	Prot	0.00	0.18	0.02	NA	0.88	0.02	NA	0.94	NA
GSN	Prot	0.00	0.18	187.88	NA	1.09	187.88	NA	1.07	NA
C3	Prot	0.00	0.19	0.04	NA	0.93	0.04	NA	0.86	NA
Glutamic acid	P-LC/MS	0.01	0.25	39.85	0.03	1.07	0.54	0.77	1.04	4.87
Unidentified	P-LC/MS	0.01	0.25	0.82	0.88	1.01	0.06	0.09	0.91	4.16
GSN	Prot	0.01	0.25	36.71	NA	1.11	36.71	NA	1.04	NA
1-Linoleoyl-L-α-lysophosphatidic acid	GC/MS	0.01	0.25	3.99	0.03	1.34	0.53	0.46	0.92	11.67
Unidentified	P-LC/MS	0.01	0.27	37.41	0.02	1.11	0.21	0.51	1.02	10.24
Coagulation factor II	Prot	0.01	0.27	0.04	NA	0.92	0.04	NA	0.85	NA
Lipid related	NMR	0.01	0.27	0.34	NA	0.83	0.34	NA	0.82	8.13
APOA2	Prot	0.01	0.27	133.80	NA	1.10	133.80	NA	1.10	NA
Unidentified	P-LC/MS	0.01	0.28	1.13	0.82	1.00	0.02	0.01	0.82	10.42
Unidentified	P-LC/MS	0.01	0.28	0.59	0.47	0.97	5.18	0.10	1.10	12.10
Pyruvic acid	GC/MS	0.01	0.28	0.34	0.02	0.69	0.35	0.17	0.72	11.04
1-Monostearinglycerol	GC/MS	0.01	0.28	19.17	0.01	1.27	0.17	0.28	0.97	9.59
Alanine	P-LC/MS	0.01	0.28	0.54	0.64	0.92	0.01	0.03	0.90	3.62
2-Ketoglutaric acid	GC/MS	0.01	0.28	0.52	0.17	0.99	0.39	0.23	0.72	25.53
APOE	Prot	0.02	0.29	19.91	NA	1.10	19.91	NA	1.17	NA
Unidentified	P-LC/MS	0.02	0.29	1.56	0.72	0.98	0.00	0.01	0.82	16.39
APOA4	Prot	0.02	0.29	0.11	NA	0.84	0.11	NA	0.89	NA
C4BPB	Prot	0.02	0.29	20.03	NA	1.10	20.03	NA	1.02	NA
Unidentified	P-LC/MS	0.02	0.29	34.80	0.05	1.03	0.24	0.52	1.04	3.28
Unidentified	NMR	0.02	0.29	0.34	NA	0.82	0.34	NA	0.88	6.64
Unidentified	P-LC/MS	0.02	0.29	0.82	0.84	0.98	0.03	0.03	0.83	13.10
HYST2477	Prot	0.02	0.29	0.14	NA	0.90	0.14	NA	1.07	NA

[a]OR, odds ratio – refers to the odds ratio estimate specific to each category obtained from the 'subset analysis'. [b]MFC, median fold change – calculated as the ratio of the median intensity among the cases to the median intensity among the controls. [c]CV estimates for metabolomics analytes are based on QC samples. For protein nodes, CV is calculated as follows. Each observed peptide ratio is normalized to the protein estimate for that sample, the protein estimate being the median of all peptides measured in that sample matching to the same protein. As these values are naturally centred around 1, the standard deviation of all the protein normalized peptide ratios is directly taken as the CV. Protein CV estimates of NA imply that the protein had only a single constituent peptide measured on all samples. FDR, false discovery rate.

observed in eight out of ten test subjects in cultures treated with 100 µM ximelagatran for 20 h compared with untreated control cells. The decreases were in the range 8–55% and displayed a clear but not statistically significant dose-dependency (Figure 1A). However, a marker for monocyte activation, HLA-DR (Figure 1B) and CD14 (Figure 1C), showed a dose-dependent increase in fluorescence intensity after ximelagatran treatment. Expression of HLA-DR increased significantly (p <0.05) after 20 h in cultures treated with 100 µM ximelagatran but not at lower concentrations. The increase of CD14 expression was significant at all tested ximelagatran concentrations (p <0.05) after 20 h in culture.

Table 3. Putative treatment-effect biomarkers.

Platform	Identification	MFC	% Change	FDR *p*-value	FDR *p*-value Wilcoxon test
NMR	3-Hydroxy butyrate	1.91	76.3	0.08	0.10
GC/MS	Pyruvic acid	0.64	-54.7	0.11	0.12
Proteomics	CSF1R	1.31	41.6	0.04	0.10
Lipid LC/MS	18:2/18:1/16:1 TG	0.48	-37.9	0.03	0.04
GC/MS	L-glutamine	0.69	-36.8	0.19	0.16
Lipid LC/MS	16:1 CE	1.40	35.6	0.02	0.04
Lipid LC/MS	52:5 TG	0.55	-35.3	0.11	0.08
GC/MS	Vitamin E	0.88	-34.7	0.20	0.18
Lipid LC/MS	18:2/18:1/18:1 TG	0.53	-32.3	0.11	0.10
Proteomics	C7 (64379)	1.27	30.9	0.12	0.18
Proteomics	coagulation factor II (64387)	0.73	-30.5	0.04	0.06
Lipid LC/MS	20:4/18:2/16:0 TG	0.68	-30.3	0.12	0.09
Lipid LC/MS	18:2/18:1/16:0 TG	0.59	-29.2	0.04	0.04
Lipid LC/MS	18:2/16:1/16:0 TG	0.50	-28.7	0.14	0.06
Proteomics	C4A variant protein	1.26	28.4	0.04	0.04
Proteomics	B2M	1.25	26.6	0.05	0.10
Lipid LC/MS	16:0/16:0 DG	0.82	-26.5	0.12	0.14
Proteomics	PROS1 (63541)	1.29	26.0	0.03	0.06
Proteomics	PROS1 (61062)	1.33	25.6	0.13	0.13
GC/MS	L-Glutamic acid	1.46	24.3	0.15	0.12
Lipid LC/MS	53:6 TG	0.68	-23.0	0.03	0.04
Polar LC/MS	Phenylalanine dimer	1.30	22.7	0.11	0.12
GC/MS	L-Phenylalanine	1.23	22.2	0.11	0.14
Proteomics	Coagulation factor II (64432)	1.24	19.8	0.10	0.14
Polar LC/MS	Phenylalanine	1.22	19.8	0.01	0.04
Lipid LC/MS	53:4 TG	0.77	-19.7	0.05	0.06
Lipid LC/MS	18:1 LPC	1.25	18.9	0.14	0.14
Proteomics	Coagulation factor II (64429)	1.22	18.7	0.04	0.06
Proteomics	C4BPA (60976)	1.12	18.6	0.07	0.10
Proteomics	Coagulation factor II (64430)	0.77	-18.2	0.03	0.04
Lipid LC/MS	18:1/18:1/16:0 TG	0.76	-18.2	0.10	0.06
Lipid LC/MS	53:3 TG	0.78	-17.7	0.14	0.12
Lipid LC/MS	18:3/18:1/18:1 TG	0.62	-17.4	0.07	0.04
Polar LC/MS	Tyrosine	1.07	16.4	0.08	0.12
Proteomics	Gc-globulin (64421)	0.86	-15.5	0.14	0.18
Proteomics	SERPINA10	1.20	15.4	0.14	0.18
Lipid LC/MS	18:1/18:1/16:0 TG	0.65	-15.3	0.15	0.08
Proteomics	RBP4	0.86	-14.9	0.02	0.04
Polar LC/MS	Glutamate	1.14	14.6	0.10	0.06
Lipid LC/MS	18:1/18:2 PC	0.80	-14.0	0.19	0.20
Polar LC/MS	Alanine	1.21	13.6	0.17	0.18
Proteomics	FCN3	1.19	13.2	0.12	0.09
Lipid LC/MS	18:1/17:1/16:0 TG	0.72	-12.4	0.19	0.12
Proteomics	C1R	1.10	11.9	0.12	0.12
Proteomics	SHBG	1.03	10.9	0.04	0.11
Proteomics	C1S	1.13	10.9	0.09	0.10
Proteomics	C2	1.11	9.6	0.07	0.10
GC/MS	Glycine-3TMS	1.10	9.4	0.14	0.12
Proteomics	CP	1.05	8.7	0.05	0.06
Proteomics	CPB2	0.90	-8.5	0.15	0.16
Proteomics	APOH	0.82	-8.0	0.15	0.12
Proteomics	FETUB	1.06	7.5	0.12	0.14
Proteomics	C7 (60034)	1.01	7.5	0.14	0.16

Table 3. continued on next page

Table 3. Continued.

Platform	Identification	MFC	% Change	FDR *p*-value	FDR *p*-value Wilcoxon test
Polar LC/MS	Glycine	1.11	7.4	0.14	0.16
Proteomics	C6	0.96	-3.0	0.14	0.16

MFC, median fold change – calculated as the ratio of the median value at the treatment time-point (pre-peak or at-peak-ALT) to the median value at the pre-dose time-point. Percentage change is calculated as percentage change in abundance relative to the pre-dose abundance (i.e. the ratio of the median of the differences in intensity between treated and pre-dose time points to the median of intensity values at the pre-dose time point). FDR, false discovery rate.

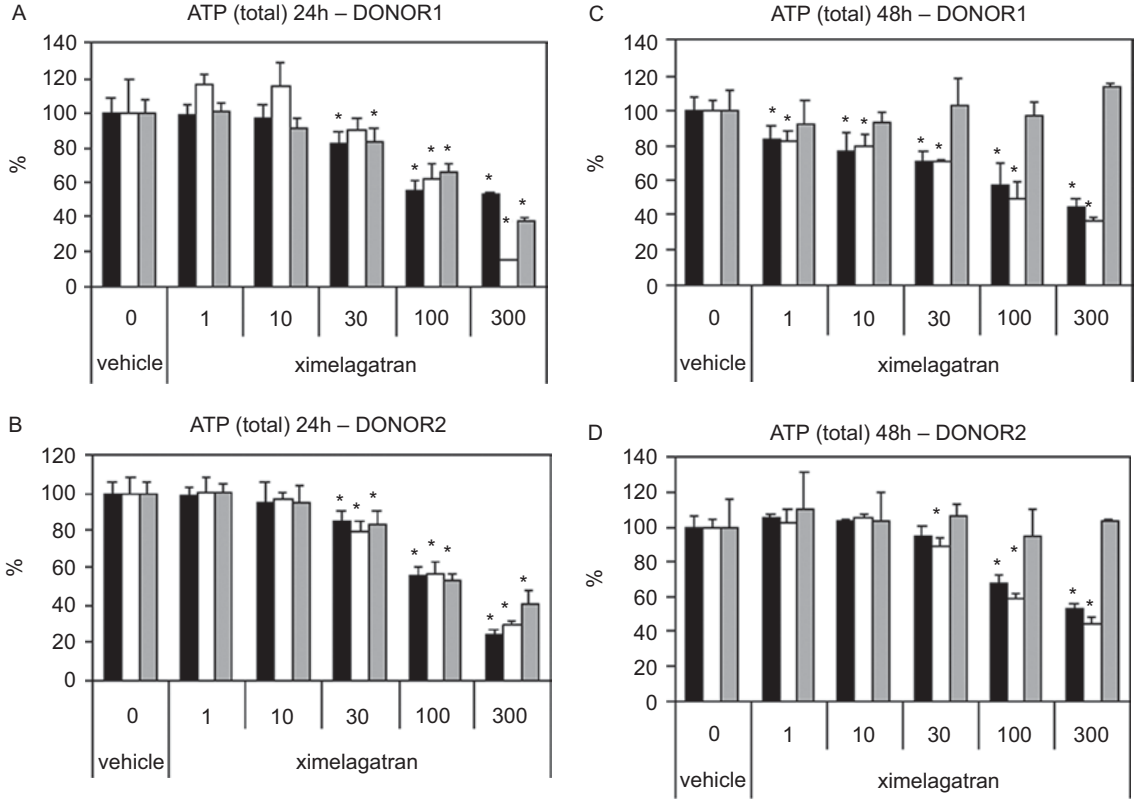

Figure 2. Total adenosine triphosphate (ATP) in primary human hepatocytes exposed to ximelagatran for (A, B) 24 h or (C, D) 48 h. ATP levels have been normalized to percentage of the value in the vehicle control groups for each pyruvate concentration. Cells were maintained in a culture medium supplemented with 0 µM (black bars), 50 µM (white bars) or 500 µM (grey) pyruvate. Data are presented as mean ± SD. *Statistically different from the control, $p < 0.05$.

The pyruvate hypothesis

The second hypothesis is based on the finding that the list of predisposition biomarkers as well as putative treatment-effect biomarkers contains many molecules involved in amino acid and TG metabolism. Pyruvate is found both in the predisposition (Table 2) and treatment-effect lists (Table 3). Plasma pyruvate levels in the pre-dose control state were analysed and ranged from 30 to 50 µM (data not shown), which is a relatively low level (Owen et al. 1980, Meierhenrich et al. 1996). Pyruvate levels were about 30% lower in cases than controls. During peak ALT elevation, the pyruvate levels were 55% lower than pre-dose cases. In addition, a 76% increase in the plasma levels of the ketone body 3-hydroxybutyrate (FDR = 0.082) was observed in the ximelagatran-treated category (Table 3). Furthermore, significantly altered TG biomarkers were mostly lower in the pre-dose case state compared with the pre-dose control state. L-Cystine had a 27% and 15% lower plasma level in the pre-dose case state in the male and female low-BMI categories, respectively (Table 2). In the ximelagatran-treated category, there was a significant reduction of L-glutamine (37%) and an increase of L-glutamic acid (24%) and glutamate (15%) in plasma.

We raised the question of whether reduced plasma levels of metabolic intermediates could exacerbate the hepatotoxicity of ximelagatran. Culturing of the human hepatoma cell line HepG2 and primary human hepatocytes was done to study if altering pyruvate levels could sensitize the cells to ximelagatran. Treatment of primary

human hepatocytes from two different donors with 1–300 µmol l^{-1} ximelagatran for either 24 or 48 h and then assay of total ATP content was carried out (Figure 2). The cells were plated in medium supplemented with 0, 50 or 500 µmol l^{-1} pyruvate in addition to that introduced in the FCS, corresponding to low, normal or high levels, respectively, relative to measured physiological concentration of pyruvate in human plasma (Mallet 2000). After 24 h exposure ximelagatran induced a dose-dependent drop in total ATP content irrespective of pyruvate concentration in the medium. By 48 h the initial drop was normalized in cells cultured in 500 µmol l^{-1} pyruvate (Figure 2, grey bars) as previously shown (Kenne et al. 2008). However, this normalization did not occur in cells that were cultured in 0 or 50 µmol l^{-1} pyruvate concentrations (Figure 2, black and white bars). To investigate whether ximelagatran could also result in cytotoxic responses in long-term treatment, primary hepatocytes were replaced with HepG2 cells. Culturing these cells in 0.5 mM glutamine in either 0 or 500 µM pyruvate did not affect their growth rate and only transiently resulted in increased LDH leakage when the cells were adapting to new culture conditions (data not shown). Cells treated with ximelagatran for 48 h did not cause any significant increase in LDH leakage until reaching a high concentration of 300 µM (Figure 3A) in either low or high pyruvate-containing medium. Importantly, ximelagatran treatment for 168 h resulted in a statistically significant ($p<0.05$) increase in LDH leakage starting at 10 µM, only in cells grown in a low-pyruvate concentration (Figure 3B). This experiment was further developed by investigating direct cell death, through membrane damage (necrosis) using the intercalating agent and fluorescent molecule, PI. HepG2 cells treated with the cytotoxic compound TBT (served as positive control) at 50 nM for 48 h, gave the same significant reduction in viability in both low- and high-pyruvate conditions (Figure 3C). However,

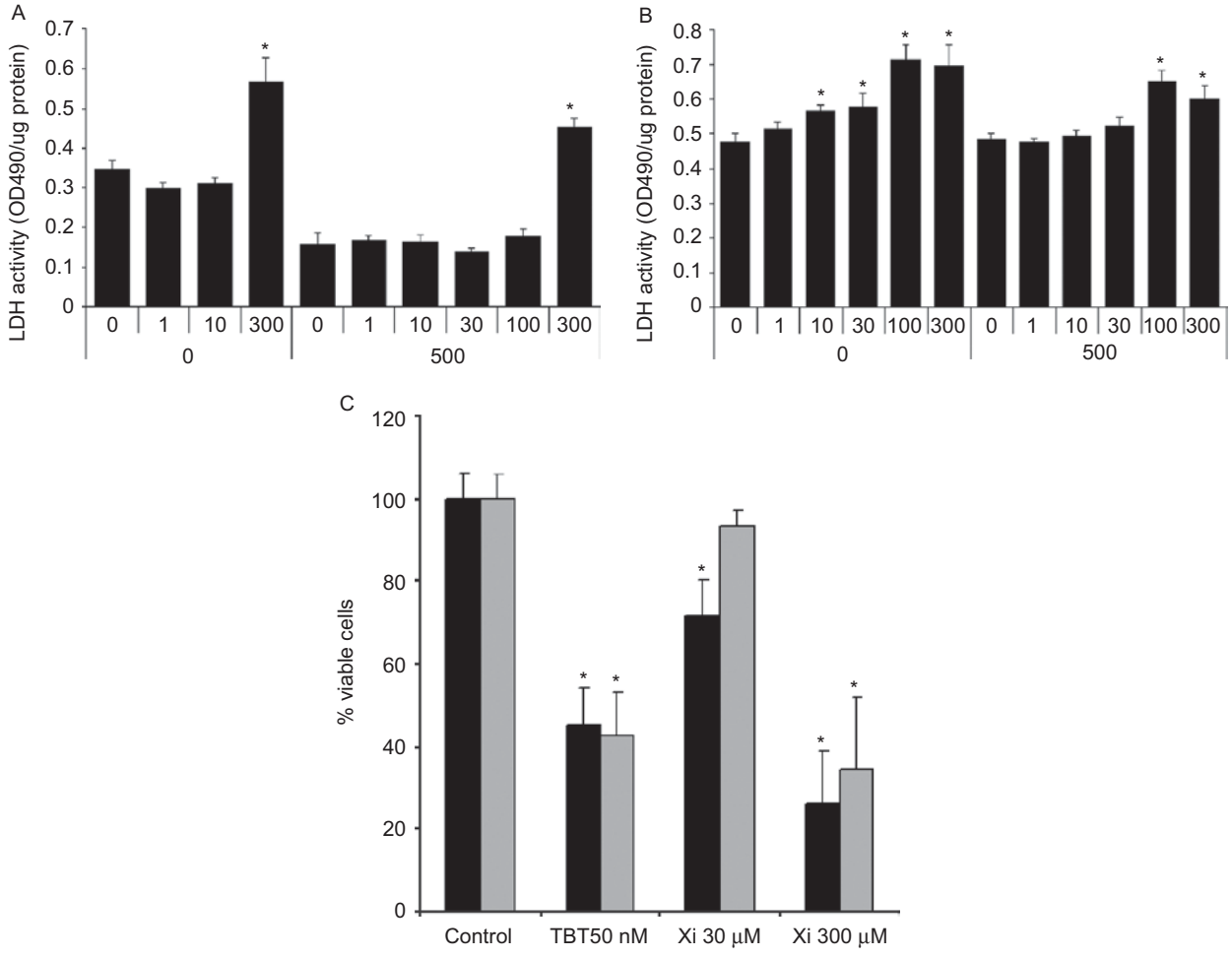

Figure 3. Lactate dehydrogenase (LDH) leakage of HepG2 cells grown in different pyruvate concentrations (0 or 500 µM) and exposed to ximelagatran for 48 h (A) or 168 h (B). Data are presented as mean + 95% confidence intervals. Percentage viable HepG2 cells (C) cultured in 0 (black bars) or 500 µM (grey bars) pyruvate medium and exposed to tributyltin (TBT, 50 nM) or ximelagatran (Xi, 30 or 300 µM) for 48 h. Diagram bars represent mean ± SD. *Statistically different from the control, $p<0.05$.

treatment with ximelgatran at 30 μM showed a statistically significant (p <0.05) decrease in cell viability only in cells cultured in a low-pyruvate medium (Figure 3C). However at higher dose of ximelagatran (300 μM) cytotoxicity was observed in cells cultured in either low- or high-pyruvate conditions and cell death pattern thus behaved as TBT treatment.

Discussion

The study presents data from a systems biology study with the objective of discovering biomarkers for predisposition to ALT increases as well as early treatment-effect biomarkers after long-term treatment with the direct thrombin inhibitor ximelagatran. Molecular profiling of proteins and endogenous metabolites was performed using a subset of samples from the SPORTIF III clinical trial. From the comprehensive lists of potential biomarker candidates presented in this article, two main hypotheses have been generated and tested *in vitro*.

Several findings indicate changes in macrophage function as having a central role in the mechanism leading to ALT elevations upon ximelagatran treatment. More specifically, these mechanisms seem to include an elevated antigen-presenting capacity indicated by increased level of CSF1R and a concomitant reduced phagocytic activity indicated by decreases in Gc-globulin and increases in C4BPA and protein S.

CSF1R is the receptor for CSF-1, a cytokine that controls the proliferation, differentiation and function of macrophages. The observed increase in plasma-derived CSF1R is an indicator of macrophage activation represented by an augmented antigen-presenting capacity of these cells (Sester et al. 1999, Dello Sbarba et al. 1996) including elevated major histocompatibility complex (MHC) class II (HLA-DR) expression. *In vitro* findings from the hypothesis-testing experiments also suggested an upregulation of MHC class II, as well as a possible CSF1R shedding after drug treatment of primary human monocytes/macrophages.

When CSF1R is shed from the cell surface, phagocytic activity is reduced, as CSF-1 can no longer bind its ligand (Chitu & Stanley 2006). Decreases in Gc-globulin could further indicate suppressed macrophage-mediated phagocytosis, as Gc-globulin plays an important role in macrophage activation (Speeckaert et al. 2006).

Increases in plasma levels of C4BPA, and protein S more specifically, reflect an inhibitory effect on phagocytosis of apoptotic cells by macrophages. Serum-derived free protein S binds to phosphatidylserine expressed on the apoptotic cell surface and stimulates the phagocytosis of apoptotic cells (Anderson et al. 2003). Once bound to the apoptotic cell surface, protein S can localize C4BPA to the cell surface forming a protein S–C4BPA complex which can inhibit the phagocytosis of apoptotic cells (Denis et al. 2005, Taylor et al. 2000, Zanni et al. 1998, Kask et al. 2004, Webb et al. 2002).

There exists a balance *in vivo* between macrophage- and dendritic cell-mediated clearance of apoptotic cells. Macrophages may maintain homeostasis by promoting the silent disposal of apoptotic cell debris, whereas clearance by dendritic cells favours an immune response (Taylor et al. 2000). As an adaptive response to this inhibition, the above balance may be tilted toward dendritic cell-mediated phagocytosis leading to an autoimmune response.

A genome-wide pharmacogenetic investigation on 74 ximelagatran cases and 130 treated controls recently revealed a strong genetic association between elevated ALT and the MHC alleles DRB1*0701 and DQA1*02, implying an important role of MHC class II (HLA-DR) in the pathogenesis, and that ximelagatran also showed specific association with soluble HLA-DR*0701-coded proteins *in vitro* (Kindmark et al. 2008). Altogether, high local drug concentrations in the liver could lead to induction of apoptotic cells. If phagocytosis is inhibited and at the same time MHC class II (HLA-DR) upregulation is achieved, the conditions for presentation of drug and/or drug cell–protein structures via a direct association with MHC, a mechanism not requiring antigen processing (Zanni et al. 1998), could be favoured. Metabolism studies of ximelagatran have not revealed any reactive metabolites or covalent binding to proteins but this does not exclude drug-specific lymphocytes from being generated (Engler et al. 2004). In support of this theory, positive lymphocyte proliferation tests have occasionally been observed in patients with elevated ALT upon ximelagatran treatment. Drug-specific cytotoxic lymphocytes could induce a local inflammatory response in the liver at the site of where the drug antigen is formed, a consequence being hepatocyte damage and an increase in ALT levels. Preferentially this would occur in subjects carrying the relevant MHC profile, in this case HLA DRB1*0701 (Kindmark et al. 2008).

While the discussion above relates primarily to non-hepatocytes, there are also effects that are most likely related to changes in hepatocyte metabolism that need to be taken into consideration. Pyruvate, a central metabolic intermediate in glucose, amino acid and lipid metabolism, is found both in the predisposition and treatment-effect lists. The level was about 30% lower in the pre-dose case state than in controls. Interestingly, the plasma pyruvate further decreased 55% in the ximelagatran-treated cases. Analysis of pyruvate concentration in representative plasma samples in the pre-dose control state suggests that the nominal plasma pyruvate concentration is around 30–50 μmol l^{-1} (data not shown). This suggests that the plasma levels may have been as low as 10 μmol l^{-1} following treatment with ximelagatran, in

the patients who experienced transaminase elevations. Low pyruvate levels and high ketone body formation would suggest a switch from hepatic lipid biosynthesis to β-oxidation. A lower plasma level of pyruvate may suggest reduced availability of pyruvate also in the liver. Acetyl-CoA formed by mitochondrial β-oxidation will either condense with oxaloacetate to form citrate (thereby entering the Krebs cycle), or condense to ketone bodies, depending on the availability of mitochondrial oxaloacetate. Because oxaloacetate is replenished by pyruvate carboxylation, reduced availability of pyruvate would be expected to favour ketone body formation. In support of this scenario, a 76% increase in the plasma levels of the 3-hydroxybutyrate was observed in the ximelagatran-treated category. 3-Hydroxybutyrate is known to increase in plasma during a low carbohydrate diet or fasting. The same metabolic state, i.e. limited availability of citric acid cycle intermediates, could also explain the lower plasma triglyceride levels in the treated case state due to inhibited hepatic TG synthesis, which is dependent upon cytosolic citrate/acetyl-CoA (Srere 1972).

In the treatment group, ximelagatran was also associated with a significant reduction in the plasma levels of glutamine, which is the most important carrier of ammonia for amino acid biosynthesis. In addition, L-cystine, which had a 27% and 15% lower plasma level in the pre-dose case state in both the male and female low-BMI categories, can be taken up by hepatocytes and converted into cysteine. Hepatic cysteine levels are a rate-limiting amino acid for hepatic glutathione (GSH) biosynthesis. It is however unclear how much is actually supplied from L-cystine in human hepatocytes *in vivo*. Further studies are needed to investigate a possible link between glutathione biosynthesis and the effects on L-cystine metabolism.

Taking all of these observations into account, it is conceivable that the limited supply of key amino acids together with a reduced supply of other key metabolic intermediates (e.g. pyruvate) may have contributed to compromised protein and in particular GSH biosynthesis and thereby increased sensitivity to the hepatocytes. This prompted us to investigate if we could demonstrate *in vitro* whether limitations in biosynthetic intermediates could exacerbate the risk of hepatotoxicity of ximelagatran. There are two independent observations from the *in vitro* experiments that support this possibility. Exposure of ximelagatran reduced ATP levels in primary human hepatocytes. This was not a cytotoxic response, but an effect that the cells recovered from, in agreement with previous observations (Kenne et al. 2008). However, ATP levels did not return to control values in the absence of high extracellular levels of pyruvate. That surprisingly suggests that ximelagatran resulted in an enhanced requirement for extracellular pyruvate, demonstrating a link between pyruvate metabolism and ximelagatran exposure, a link that was also suggested by the clinical samples. Because primary human hepatocytes are unsuitable for experiments requiring longer time in culture (because of variable viability of primary hepatocytes) we changed to the human hepatoma cell line HepG2 and propagated these cells in low (<10 μM, only source of pyruvate from FCS), normal (50 μM) or high (500 μM) concentrations of pyruvate. Irrespective of pyruvate concentration, these cells demonstrated cytotoxic effects at 300 μM ximelagatran following 48 h exposure, in agreement with previous findings from our laboratory (Kenne et al. 2008).

However, when HepG2 cells were kept in culture in low pyruvate levels for longer treatment with ximelagatran this resulted in increased LDH leakage already at 10–30 μM. These concentrations (10 μM) of ximelagatran may be relevant for the clinical situation. In patients receiving oral ximelagatran 36 mg twice daily, the mean peak plasma concentration (C_{max}) was 0.3 μM for ximelgatran (Wolzt et al. 2003). Based upon the whole body distribution of radiolabelled ximelagatran in rats, maximum concentrations of ximelagatran were up to 20 times higher in the liver than in plasma (Kenne et al. 2008).

Using the sensitive method of PI staining, it was possible to demonstrate a cytotoxic effect in HepG2 cells of ximelagatran at 30 μM in pyruvate-free medium already after 48 h treatment. In addition, there was no cytotoxicity caused by ximelagatran at 10–30 μM when HepG2 cells were cultured in high concentrations of pyruvate using either LDL or PI staining as detection methods.

At present we can only speculate as to the mechanism behind this hepatotoxic response to ximelagatran and why this effect was only observed when cells were cultured in a medium with limited availability of metabolic intermediates, but it is possible that an insufficient supply of pyruvate, cytosolic acetyl-CoA and glutamine, all of which are key intermediates in amino acid metabolism results in hepatic amino acid deprivation (Figure 4). This could trigger activation of the protein kinase GCN2, which senses low levels of amino acid (Zhang et al. 2002). This in turns initiates a potentially cytotoxic stress response, involving inhibition of protein and fatty acid synthesis (Guo & Cavener 2007), the latter clearly supported by the plasma lipid analysis in the present study.

Figure 4 illustrates a scenario where predisposing factors in conjunction with altered amino acid usage results in amino acid deprivation and cellular stress, which eventually could result in increased hepatocyte necrosis and/or apoptosis.

A hepatotoxic response attributed to amino acid deprivation has been described in animals treated with L-asparaginase. A drop in serum glutamine, in the same magnitude as observed in this study, resulted

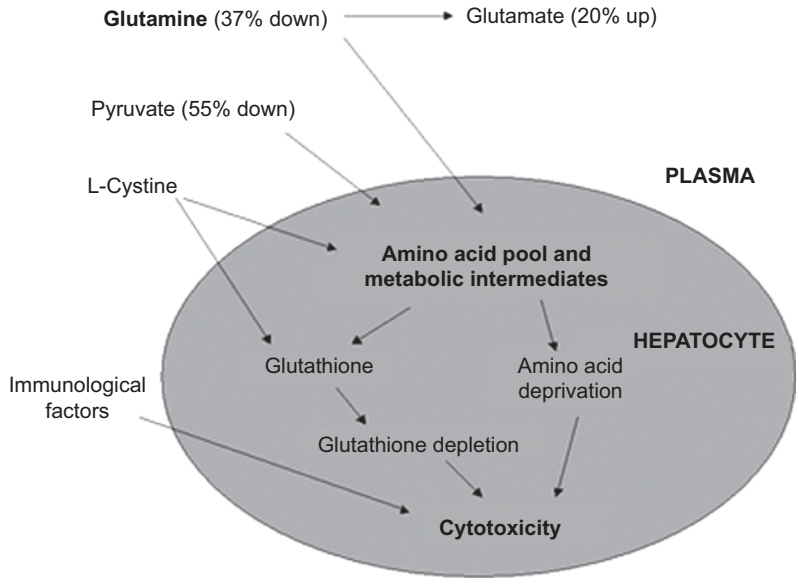

Figure 4. A proposed model of predisposing and treatment factors in conjunction with altered amino acid usage results in amino acid deprivation and cellular stress, which eventually could result in increased hepatocyte cell death in susceptible individuals. Possible treatment effect on glutamine, glutamate and pyruvate are presented in brackets.

in hepatotoxicity mediated via GCN2 activation and eIF2α phosphorylation. If the contaminating glutaminase activity was removed from the L-asparaginase preparation, there was no hepatic amino acid deprivation or cell stress (Reinert et al. 2006). Similarly, panadiplon, an experimental non-benzodiazepine anxiolytic, produced evidence of hepatic toxicity in phase I clinical trial volunteers that was not predicted by rat, dog or monkey preclinical studies. Subsequent studies showed that a carboxylic acid metabolite of panadiplon caused a redistribution of the cellular coenzyme A stores and inhibition of β-oxidation, rendering hepatocytes sensitive to secondary stress (e.g. hypoxia), which subsequently produced apoptosis and hepatocellular necrosis (Ulrich et al. 2001). It was shown *in vitro* that co-treatment with pyruvate reduced the level of LDH leakage caused by panadiplon under hypoxic conditions (Bacon et al. 1996). Our data showed that ximelagatran treatment resulted in a drop in ATP levels in primary hepatocytes and increased LDH leakage in HepG2 cells when the cells were cultured with limited availability to pyruvate. The treatment induced a reduction in pyruvate levels which suggest that ximelagatran can enhance the utilization of pyruvate as a metabolic intermediate. Ximelagatran does not inhibit fatty acid β-oxidation (Kenne et al. 2008), but nevertheless the drop in plasma pyruvate could reflect an increased demand of pyruvate. This may proceed to a point where glycolytically produced pyruvate is insufficient to meet demand. Whether pyruvate is consumed in anaerobic ATP production, gluconeogenesis, anaplerosis or some other metabolic pathway is currently unclear. Preliminary experiments in our laboratory, have shown that ximelagatran induces gene expression of both PEPCK and PDK4 both in primary human hepatocytes and HepG2 cells (data not shown), suggesting that treatment redirects pyruvate to gluconeogenesis (Sugden & Holness 2006). For instance, pyruvate could be used in the production of glucose 6-phosphate through gluconeogenesis that could be subsequently used in the pentose phosphate shunt in order to maintain high levels of reducing equivalents (NAPDPH).

The metabolome profile in predisposed patients, together with the treatment-related effects, could suggests that the sensitive patients could have been undernourished and at some stage of muscle wasting prior and during the treatment. Undernourishment is a surprisingly common and potentially life-threatening situation in the elderly and often remains undiagnosed. According to Silver (1991), undernutrition ranges from 5 to 12% in the community-dwelling elderly. This condition does not necessarily exclude obese individuals, who could by definition be considered malnourished, but they are likely to have a somewhat different metabolome profile.

A protective effect of pyruvate against plasma ALT elevation might also stem from the fact that pyruvate is an effective reactive oxygen species scavenger. Cytoprotective effects of pyruvate against oxidative stress in biological systems have been reported (O'Donnell-Tormey et al. 1987, Desagher et al. 1997, Tsung et al. 2005, Hinoi et al. 2006, Wang & Cynader 2001). For example, ethyl pyruvate, a soluble pyruvate derivative, has a protective effect on hepatic ischemia-reperfusion

injury and paraquat-intoxicated rats mediated in part by decreasing lipid peroxidation, downregulation of inflammatory mediators, and inhibition of hepatic apoptosis and necrosis (Lee et al. 2008, Tsung et al. 2005). An alternative mechanism explaining the decreased pyruvate levels in patients treated with ximelagatran is the significant increase in ALT activity, resulting from the release of ALT from damaged hepatocytes. ALT enzyme in plasma may utilize plasma pyruvate or glutamate as enzymatic substrates (reverse ALT reaction), yielding alanine or α-ketoglutarate, respectively. While there was a slight increase in plasma alanine concomitantly with a drop in pyruvate levels, the treatment related changes in glutamate and α-ketoglutarate in treatment samples does not favour this mechanism. In addition, this hypothesis cannot explain why pyruvate was a predisposition marker.

The value of the biological hypothesis for the basis of predisposition to ALT elevations during ximelagatran treatment and the statistical confidence in the biomarker sets from which the hypotheses were developed are limited by the lack of samples from ximelagatran-treated normal subjects as well as the heterogeneity in the study subjects with respect to their disease status, gender, BMI and other unknown factors (e.g. race/ethnicity, study site, etc.). Furthermore, the lack of time point-matched samples from treated controls during ximelagatran treatment (i.e. patients who did not exhibit ALT elevation >3xULN during treatment) makes it impossible to separate a toxicity response from a pharmacological response and limits the strength of any hypothesis concerning the relationship of ximelagatran treatment-effect biomarkers to liver damage and resulting ALT elevations. Future studies will focus on a larger clinical trial (e.g. SPORTIF V) for targeted analysis of key metabolites/proteins found in the present work to improve the statistical power.

This study was performed on available samples from a clinical trial that was not designed for biomarker research in terms of samples types, longitudinal sampling or number of patients. However, the combination of multiple platforms for endogenous metabolite and protein analysis has contributed highly to the generation of the hypotheses.

The concept of systems biology has clearly been proven successful in increasing our understanding of unknown mechanisms of toxicity, and could help building hypotheses that could advance translational and personalized medicine in the future.

Acknowledgements

We would like to thank Ingela Gustafsson and Ingalill Rafter for excellent technical assistance and Johan Lengqvist for help with the text of analytical platforms.

Declaration of interest: The authors report no conflicts of interest. The authors alone are responsible for the content and writing of the paper.

References

Ambroise C, McLachlan GJ. (2002). Selection bias in gene extraction on the basis of microarray gene-expression data. Proc Natl Acad Sci U S A 99:6562–6.

Anderson HA, Maylock CA, Williams JA, Paweletz CP, Shu H, Shacter E. (2003). Serum-derived protein S binds to phosphatidylserine and stimulates the phagocytosis of apoptotic cells. Nat Immunol 4:87–91.

Bacon JA, Cramer CT, Petrella DK, Sun EL, Ulrich RG. (1996). Potentiation of hypoxic injury in cultured rabbit hepatocytes by the quinoxalinone anxiolytic panadiplon. Toxicology 108:9–16.

Benjamini Y, Hochberg Y. (1995). Controlling the false discovery rate: a practical and powerful approach to multiple testing. J R Stat Soc 57:289–300 (Abstract).

Breiman L. (2001). Random Forests. Machine Learning 45:5–32 (Abstract).

Chitu V, Stanley ER. (2006). Colony-stimulating factor-1 in immunity and inflammation. Curr Opin Immunol 18:39–48.

Davidov E, Clish CB, Oresic M, Meys M, Stochaj W, Snell P, Lavine G, Londo TR, Adourian A, Zhang X, Johnston M, Morel N, Marple EW, Plasterer TN, Neumann E, Verheij E, Vogels JT, Havekes LM, van der Greef J, Naylor S. (2004). Methods for the differential integrative omic analysis of plasma from a transgenic disease animal model. OMICS 8:267–88.

Dello Sbarba P, Nencioni L, Labardi D, Rovida E, Caciagli B, Cipolleschi MG. (1996). Interleukin 2 down-modulates the macrophage colony-stimulating factor receptor in murine macrophages. Cytokine 8:488–94.

Denis CV, Roberts SJ, Hackeng TM, Lenting PJ. (2005). In vivo clearance of human protein S in a mouse model: influence of C4b-binding protein and the Heerlen polymorphism. Arterioscler Thromb Vasc Biol 25:2209–15.

Desagher S, Glowinski J, Premont J. (1997). Pyruvate protects neurons against hydrogen peroxide-induced toxicity. J Neurosci 17:9060–7.

Engler OB, Strasser I, Naisbitt DJ, Cerny A, Pichler WJ. (2004). A chemically inert drug can stimulate T cells in vitro by their T cell receptor in non-sensitised individuals. Toxicology 197:47–56.

Guo F, Cavener DR. (2007). The GCN2 eIF2alpha kinase regulates fatty-acid homeostasis in the liver during deprivation of an essential amino acid. Cell Metab 5:103–14.

Hinoi E, Takarada T, Tsuchihashi Y, Fujimori S, Moriguchi N, Wang L, Uno K, Yoneda Y. (2006). A molecular mechanism of pyruvate protection against cytotoxicity of reactive oxygen species in osteoblasts. Mol Pharmacol 70:925–35.

Kask L, Trouw LA, Dahlback B, Blom AM. (2004). The C4b-binding protein–protein S complex inhibits the phagocytosis of apoptotic cells. J Biol Chem 279:23869–73.

Kenne K, Skanberg I, Glinghammar B, Berson A, Pessayre D, Flinois JP, Beaune P, Edebert I, Pohl CD, Carlsson S, Andersson TB. (2008). Prediction of drug-induced liver injury in humans by using in vitro methods: the case of ximelagatran. Toxicol In Vitro 22:730–46.

Kindmark A, Jawaid A, Harbron CG, Barratt BJ, Bengtsson OF, Andersson TB, Carlsson S, Cederbrant KE, Gibson NJ, Armstrong M, Lagerstrom-Fermer ME, Dellsen A, Brown EM, Thornton M, Dukes C, Jenkins SC, Firth MA, Harrod GO, Pinel TH, Billing-Clason SM, Cardon LR, March RE. (2008). Genome-wide pharmacogenetic investigation of a hepatic adverse event without clinical signs of immunopathology suggests an underlying immune pathogenesis. Pharmacogenomics J 8:186–95.

Koek MM, Muilwijk B, van der Werf MJ, Hankemeier T. (2006). Microbial metabolomics with gas chromatography/mass spectrometry. Anal Chem 78:1272–81.

Lee J, Kwon W, Jo Y, Suh G, Youn Y. (2008). Protective effects of ethyl pyruvate treatment on paraquat-intoxicated rats. Hum Exp Toxicol 27:49–54.

Lee WM. (2003). Drug-induced hepatotoxicity. N Engl J Med 349:474–85.

Lee WM, Larrey D, Olsson R, Lewis JH, Keisu M, Auclert L, Sheth S. (2005). Hepatic findings in long-term clinical trials of ximelagatran. Drug Saf 28:351–70.

Mallet RT. (2000). Pyruvate: metabolic protector of cardiac performance. Proc Soc Exp Biol Med 223:136–48.

McCaffrey E, Brown S. (2006). AstraZeneca decides to withdraw Exanta™ http://www.astrazeneca.com/pressrelease/5217.aspx.

Meierhenrich R, Jedicke H, Voigt A, Lange H. (1996). The effect of erythropoietin on lactate pyruvate and excess lactate under physical exercise in dialysis patients. Clin Nephrol 45:90–7.

O'Donnell-Tormey J, Nathan CF, Lanks K, DeBoer CJ, de la Harpe J. (1987). Secretion of pyruvate. An antioxidant defense of mammalian cells. J Exp Med 165:500–14.

Olsson SB; Executive Steering Committee of the SPORTIF III Investigators. (2003). Stroke prevention with the oral direct thrombin inhibitor ximelagatran compared with warfarin in patients with non-valvular atrial fibrillation (SPORTIF III): randomised controlled trial. Lancet 362:1691–8.

Owen OE, Mozzoli MA, Boden G, Patel MS, Reichard GA Jr, Trapp V, Shuman CR, Felig P. (1980). Substrate hormone and temperature responses in males and females to a common breakfast. Metabolism 29:511–23.

Reinert RB, Oberle LM, Wek SA, Bunpo P, Wang XP, Mileva I, Goodwin LO, Aldrich CJ, Durden DL, McNurlan MA, Wek RC, Anthony TG. (2006). Role of glutamine depletion in directing tissue-specific nutrient stress responses to L-asparaginase. J Biol Chem 281:31222–33.

Ross PL, Huang YN, Marchese JN, Williamson B, Parker K, Hattan S, Khainovski N, Pillai S, Dey S, Daniels S, Purkayastha S, Juhasz P, Martin S, Bartlet-Jones M, He F, Jacobson A, Pappin DJ. (2004). Multiplexed protein quantitation in Saccharomyces cerevisiae using amine-reactive isobaric tagging reagents. Mol Cell Proteomics 3:1154–69.

Sester DP, Beasley SJ, Sweet MJ, Fowles LF, Cronau SL, Stacey KJ, Hume DA. (1999). Bacterial/CpG DNA down-modulates colony stimulating factor-1 receptor surface expression on murine bone marrow-derived macrophages with concomitant growth arrest and factor-independent survival. J Immunol 163:6541–50.

Silver AJ. (1991). Malnutrition. In: Geriatrics Review Syllabus. A Core Curriculum in Geriatric Medicine. New York: American Geriatrics Society.

Speeckaert M, Huang G, Delanghe JR, Taes YE. (2006). Biological and clinical aspects of the vitamin D binding protein (Gc-globulin) and its polymorphism. Clin Chim Acta 372:33–42.

Srere PA. (1972). The citrate enzymes: their structures mechanisms and biological functions. Curr Top Cell Regul 5:229–83.

Sugden MC, Holness MJ. (2006). Mechanisms underlying regulation of the expression and activities of the mammalian pyruvate dehydrogenase kinases. Arch Physiol Biochem 112:139–49.

Taylor PR, Carugati A, Fadok VA, Cook HT, Andrews M, Carroll MC, Savill JS, Henson PM, Botto M, Walport MJ. (2000). A hierarchical role for classical pathway complement proteins in the clearance of apoptotic cells in vivo. J Exp Med 192:359–66.

Tsung A, Kaizu T, Nakao A, Shao L, Bucher B, Fink MP, Murase N, Geller DA. (2005). Ethyl pyruvate ameliorates liver ischemia-reperfusion injury by decreasing hepatic necrosis and apoptosis. Transplantation 79:196–204.

Ulrich RG, Bacon JA, Brass EP, Cramer CT, Petrella DK, Sun EL. (2001). Metabolic idiosyncratic toxicity of drugs: overview of the hepatic toxicity induced by the anxiolytic panadiplon. Chem Biol Interact 134:251–70.

van der Greef J, Martin S, Juhasz P, Adourian A, Plasterer T, Verheij ER, McBurney RN. (2007). The art and practice of systems biology in medicine: mapping patterns of relationships. J Proteome Res 6:1540–59.

Vandesompele J, De Preter K, Pattyn F, Poppe B, Van Roy N, De Paepe A, Speleman F. (2002). Accurate normalization of real-time quantitative RT-PCR data by geometric averaging of multiple internal control genes. *Genome Biol* 3:RESEARCH0034

Wald P. (1949). Note on the consistency of the maximum likelihood estimate. The Ann Math Stat 20:595–601 (Abstract).

Wang XF, Cynader MS. (2001). Pyruvate released by astrocytes protects neurons from copper-catalyzed cysteine neurotoxicity. J Neurosci 21:3322–31.

Webb JH, Blom AM, Dahlback B. (2002). Vitamin K-dependent protein S localizing complement regulator C4b-binding protein to the surface of apoptotic cells. J Immunol 169:2580–6.

Wolzt M, Wollbratt M, Svensson M, Wahlander K, Grind M, Eriksson UG. (2003). Consistent pharmacokinetics of the oral direct thrombin inhibitor ximelagatran in patients with nonvalvular atrial fibrillation and in healthy subjects. Eur J Clin Pharmacol 59:537–43.

Zanni MP, von Greyerz S, Schnyder B, Brander KA, Frutig K, Hari Y, Valitutti S, Pichler WJ. (1998). HLA-restricted processing- and metabolism-independent pathway of drug recognition by human alpha beta T lymphocytes. J Clin Invest 102: 1591–8.

Zhang P, McGrath BC, Reinert J, Olsen DS, Lei L, Gill S, Wek SA, Vattem KM, Wek RC, Kimball SR, Jefferson LS, Cavener DR. (2002). The GCN2 eIF2alpha kinase is required for adaptation to amino acid deprivation in mice. Mol Cell Biol 22:6681–8.